Pairing Dynamics of Polar States in a Quenched p-wave Superfluid Fermi Gas

Sukjin Yoon[1, 2] and Gentaro Watanabe[1, 3, 4, 5]

[1] *Asia Pacific Center for Theoretical Physics (APCTP), Pohang, Gyeongbuk 37637, Korea*
[2] *Quantum Universe Center, Korea Institute for Advanced Study, Seoul 02455, Korea*
[3] *Department of Physics, POSTECH, Pohang, Gyeongbuk 37673, Korea*
[4] *Center for Theoretical Physics of Complex Systems, IBS, Daejeon 34051, Korea*
[5] *University of Science and Technology, Daejeon 34113, Korea*

(Dated: December 31, 2015)

We consider polar states of a single-species superfluid Fermi gas tuned close to a p-wave Feshbach resonance of $m = 0$ projection in 3 dimensions and investigate their pairing dynamics after a sudden change of interaction strength. The time evolution of the pairing field, momentum distribution, and pair amplitude distribution is obtained numerically within a mean-field approach. The anisotropy of pair interaction together with the presence of the centrifugal barrier results in different pairing dynamics compared to the s-wave case. Depending on the initial state, quench to BCS regime results in interconversion of atomic and resonant states, molecular and atomic states, or BCS-paired and atomic states, via resonant state of the final Hamiltonian. This leads to narrow oscillatory hole-burning (large depletion of momentum occupation) inside the Fermi sea or particle-peak (large filling of momentum occupation) at different rate depending on the polar angle from the symmetry axis in momentum space. The frequency of decaying oscillation of the pairing field agrees with that of oscillatory hole-burning/particle-peak on the symmetry axis.

PACS numbers: 03.75.Kk, 03.75.Ss, 05.30.Fk

arXiv:1512.09058v1 [cond-mat.quant-gas] 30 Dec 2015

Introduction. - The unprecedented control over the cold gases with tunable interactions via Feshbach resonances (FRs) has mapped new landscape of superfluidity and has given impetus to study the nature of the symmetry-broken state. While the amplitude mode, referred to as the Higgs mode, of the order parameter was anticipated to appear in a superconductor in response to a small perturbation in non-adiabatic regime [1], recent resurgent studies on the amplitude modes of the order parameters have been motivated from new prospects in cold atomic gases: the large dynamical time-scale and high controllability of the cold atomic gases have made quantum quench, sudden change of system's parameter(s), become a practical subject of experimental control as well as theoretical investigation and provided us unprecedented opportunities of studying the subsequent non-equilibrium dynamics. For the last decade, the coherent dynamics of the order parameter, induced by quantum quenches in s-wave Fermi gases has been investigated and classified [2–10].

Finite angular-momentum paired atomic superfluids are compelling because they are or may be connected to superfluid ^{3}He [11], neutron superfluid inside neutron stars [12], high-T_c superconductors, and the topological features (in 2 dimensions) useful for the quantum computing [13, 14]. p-wave paired atomic gases can exhibit distinct phases of superfluidity characterized by their rich order parameter as a function of temperature and interaction strength [15, 16]. These phases and the phase transitions between them can be accessible via detuning between BCS and Bose-Einstein condensation (BEC) limits with a p-wave FR. Although p-wave FRs have already been realized in experiments [17–21], obtaining stable p-wave atomic superfluids has been challenging due to inelastic collisional losses [22] and has not been achieved in laboratories yet. Since there have been efforts or proposals [23–30] to overcome or circumvent the obstacles and quench process might be used as part of an experimental operation to obtain the desired state [24], it is worthwhile to consider the dynamical behaviors of the p-wave paired superfluid states after quantum quench. The quench dynamics of topological superfluid axial $(p_x + ip_y)$ states has been discussed in the spin-orbit-coupled superfluid Fermi gas in 2 dimensions [31–33].

In this paper, we consider polar (p_x) states of a single-species p-wave superfluid Fermi gas in 3 dimensions at zero temperature and investigate their pairing dynamics after a sudden change in the interaction strength which is tunable close to a p-wave FR of $m = 0$ projection. Dynamics of the pairing field including the momentum distribution and the pair amplitude distribution in momentum space is obtained numerically within a mean-field (MF) approach. Our findings are as follows: the anisotropy of the p-wave paired polar states together with the presence of the centrifugal barrier gives rise to the pairing dynamics qualitatively different from the s-wave Fermi gas. When the interaction is quenched to BCS side either from BCS or from BEC side, a centrifugal barrier supports resonant molecular states at the final strength of the interaction. (1) When the interaction is changed to a value of stronger attraction within BCS regime, interconversion between atomic and resonant states appears and the resulting oscillatory hole-burning (large depletions in momentum distribution) is at different rate depending on the polar angle from the symmetry axis. (2) When the interaction is changed to a value of weaker attraction within BCS regime or changed from BEC regime to BCS regime, interconversion between BCS-paired and

resonant states or between molecular and resonant states appears via the resonant state of the final Hamiltonian, which leads to the oscillatory particle-peak (large filling in the momentum distribution) with conversion rate depending on the polar angle from the symmetry axis. (3) The decaying oscillation frequency of the pairing field agrees with hole-burning/particle-peak frequency on the symmetry axis. This is connected to the observation that pair amplitudes in the region of hole-burning/particle-peak located off the symmetry axis in momentum space display a phase structure like a vortex-ring while those on the symmetry axis cannot topologically.

Model and Formulation. - We consider a single-species polarized Fermi gas with a p-wave interaction $V_1(\mathbf{k},\mathbf{k}')$,

$$H = \sum_{\mathbf{k}} \xi_k \hat{a}^\dagger_{\mathbf{k}} \hat{a}_{\mathbf{k}} + \frac{1}{2} \sum_{\mathbf{k},\mathbf{k}',\mathbf{q}} V_1(\mathbf{k},\mathbf{k}') \hat{b}^\dagger_{\mathbf{k},\mathbf{q}} \hat{b}_{\mathbf{k}',\mathbf{q}} \ , \quad (1)$$

where $\hat{a}^\dagger_{\mathbf{k}}$ creates a fermion atom of momentum $\mathbf{k}$, $\xi_k = k^2/2M - \mu$ with M the atom mass and μ the chemical potential, and $\hat{b}^\dagger_{\mathbf{k},\mathbf{q}} = \hat{a}^\dagger_{\mathbf{k}+\mathbf{q}/2} \hat{a}^\dagger_{-\mathbf{k}+\mathbf{q}/2}$. The Pauli principle excludes the possibility of s-wave channel interaction for a single-species Fermi gas and we introduce the dominant p-wave attractive interaction potential of a separable form

$$V_1(\mathbf{k},\mathbf{k}') = -4\pi g \Gamma^*_m(\mathbf{k}) \Gamma_m(\mathbf{k}') \quad (2)$$

with

$$\Gamma_m(\mathbf{k}) = \frac{k k_0}{k^2 + k_0^2} Y_{1,m}(\hat{\mathbf{k}}) \ , \quad (3)$$

where g (> 0) is a coupling strength, m is the angular momentum projection, and k_0 is a momentum cutoff [34, 35].

In the p-wave FR, the dipolar anisotropy splits FR into a doublet of $m = \pm 1$ and $m = 0$ resonances [17]. In the case of large dipolar splitting, the system can be independently tuned into $m = 0$ and $m = \pm 1$ resonances displaying axial ($p_x + ip_y$) and polar (p_x) states separately [15, 16]. We consider a p-wave FR of $m = 0$ projection: $\Gamma_0(\mathbf{k}) = \frac{k k_0}{k^2+k_0^2} Y_{1,0}(\hat{\mathbf{k}})$ where $Y_{1,0}(\hat{\mathbf{k}}) = \sqrt{3/4\pi}\cos\theta$.

The low energy scattering amplitude for the p-wave channel $f_1(k) = k^2 / \left(-\frac{1}{a_p} + \frac{r_p k^2}{2} - ik^3\right)$ is obtained provided g and k_0 are related to the two parameters (a_p is scattering volume and r_p has dimension of inverse length): $\frac{1}{4\pi g} = -\frac{MV}{16\pi^2 a_p k_0^2} + \sum_k \frac{|\Gamma_0(k)|^2}{2\epsilon(k)}$ and $r_p = -\frac{1}{k_0}\left(k_0^2 + \frac{4}{k_0 a_p}\right)$ as in [34]. The pole of the scattering amplitude is given by $E_{\rm pole} = 2/M a_p r_p$ which corresponds to a bound state for $a_p < 0$ and a resonant state (due to a centrifugal barrier) for $a_p > 0$.

We employ the mean-field approximation for pairing between atoms of equal and opposite momenta (see [15] for the argument on the reliability of this approximation in p-wave Fermi gases of low density). The time evolution of our system is described by the time-dependent

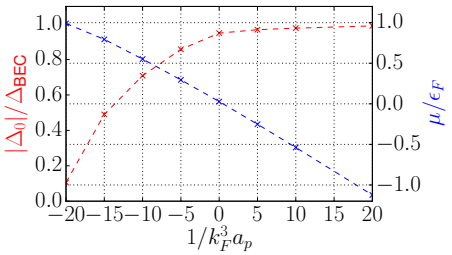

FIG. 1: Equlibrium values of μ and $|\Delta_0|$ as a function of inverse scattering volume $1/a_p$.

Bogoliubov-de Gennes (BdG) equations

$$i\frac{\partial}{\partial t}\begin{pmatrix} u_{\mathbf{k}}(t) \\ v_{\mathbf{k}}(t) \end{pmatrix} = \begin{pmatrix} \xi_{\mathbf{k}} & \Delta_{\mathbf{k}}(t) \\ \Delta^*_{\mathbf{k}}(t) & -\xi_{\mathbf{k}} \end{pmatrix} \begin{pmatrix} u_{\mathbf{k}}(t) \\ v_{\mathbf{k}}(t) \end{pmatrix} \ , \quad (4)$$

where $u_{\mathbf{k}}(t)$ and $v_{\mathbf{k}}(t)$ are quasiparticle amplitudes and the pairing field $\Delta_{\mathbf{k}}(t)$ is given by

$$\Delta_{\mathbf{k}}(t) = \sum_{\mathbf{k}'} V_1(\mathbf{k},\mathbf{k}') u^*_{\mathbf{k}'}(t) v_{\mathbf{k}'}(t) \ . \quad (5)$$

In our potential of separable form, $\Delta_{\mathbf{k}} = \Gamma_0(\mathbf{k})\Delta_0 = \Gamma_0(\mathbf{k})(-4\pi g \sum_{\mathbf{k}'} \Gamma_0(\mathbf{k}') u^*_{\mathbf{k}'} v_{\mathbf{k}'})$. For convenience, we call $|\Delta_0|$ as a pairing amplitude even though the actual pairing amplitude $|\Gamma_0(\mathbf{k})\Delta_0|$ has a momentum dependence. The anisotropic nature of $\Gamma_0(\mathbf{k})$ plays a role in the pairing dynamics as we can see shortly.

In our discussion, we assume that gas sample of size L is smaller than the coherence length ξ and neglect inhomogeneous phase fluctuations and vortices. Our initial state is prepared in the ground state at an initial scattering volume $(a_p)_{\rm init}$ and the scattering volume is changed suddenly to a final value $(a_p)_{\rm fin}$.

Results. - We choose $k_0 = 40 k_F$ where $k_0/k_F \gg 1$ is satisfied for the diluteness of the gas. The parameter r_p does not change much during the quench processes discussed below and we safely fix the value of r_p at the initial value during the time evolution.

Equilibrium properties of polar states from BCS to BEC regime were studied in [35] and our parameters give qualitatively the same behavior as shown in Fig. 1. $k_F = (6\pi^2 N/V)^{1/3}$, $\epsilon_F = k_F^2/2M$, and $\Delta_{\rm BEC} = 8\epsilon_F (0.5 k_0^2/9\epsilon_F)^{1/4} \approx 29.2\epsilon_F$ is the asymptotic value of the pairing amplitude $|\Delta_0|$ in the BEC limit.

First, we consider the case that $1/k_F^3 a_p$ is quenched to the value of stronger attraction (hereafter, called "forward quench"): (a) BCS $\to$ BCS ($1/k_F^3 a_p$: $-20 \to -10$), (b) BCS $\to$ BEC ($1/k_F^3 a_p$: $-20 \to +10$), and (c) BEC $\to$ BEC ($1/k_F^3 a_p$: $+5 \to +20$). The dynamics of the pairing amplitude $|\Delta_0|$ and the momentum distribution $|v_{\mathbf{k}}|^2 (k_z = 0)$ at the local maximum (in time domain) of the pairing field are shown in Fig. 2. The dynamics in the case of quench within BEC regime ($1/k_F^3 a_p : +5 \to +20$) is not shown because $|\Delta_0|$ is almost saturated in the BEC side and there is no noticeable pairing dynamics. Only the first quadrant of k_x-k_y plane is shown due to the az-

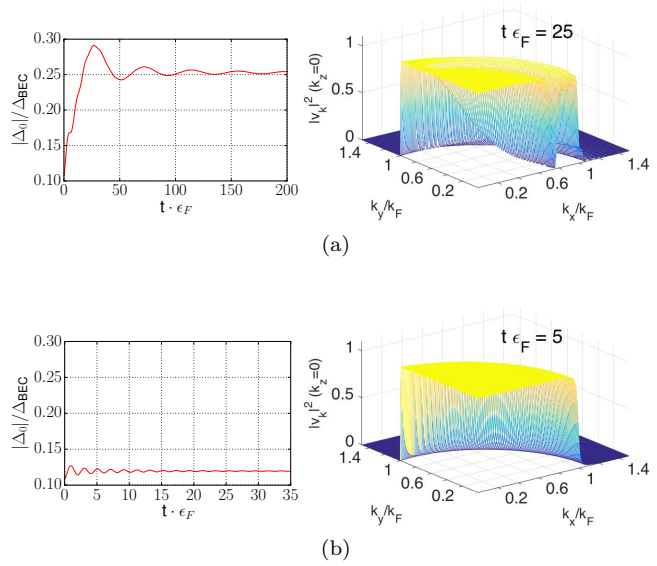

FIG. 2: Dynamics of $|\Delta_0|$ and the momentum occupation $|v_{\mathbf{k}}|^2$ at the designated time. Inverse scattering volume $1/k_F^3 a_p$ is quenched (a) from -20 to -10 and (b) from -20 to 10.

imuthal symmetry about k_x-axis and the reflection symmetry on the k_y-k_z plane.

In case (a), large depletion of momentum occupation inside the Fermi sea (called "hole-burning") is observed and it is connected to a large time-scale oscillation (on top of it, a short time-scale decaying oscillation of small amplitude is seen at the early stage up till $t = 25/\epsilon_F$ or so) of $|\Delta_0|$. The hole-burning point is at $k = k_h$ satisfying $k_h^2/2M \approx 0.5\epsilon_F \approx E_r/2$ where E_r is the resonant state energy at the final value of $1/k_F^3 a_p$. The location of the hole-burning point is independent of the initial states of $1/k_F^3 a_p = -20$, -15, and -10 as far as tested.

The anisotropy of the p-wave pairing field ($\Delta_{\mathbf{k}}(t) \propto \cos\theta$) makes the hole-burning rate slow down as the polar angle from the symmetry axis (k_x-axis) increases and hole-burning appears as in Fig. 2 (a) at the early stage of $t \cdot e_F = 25$. Figure 3 shows the density plots of case (a) in Fig. 2 at $t \cdot e_F = 25$ (left) and 60 (right). It seems that a hole-burning region created on the k_x- axis evolves into

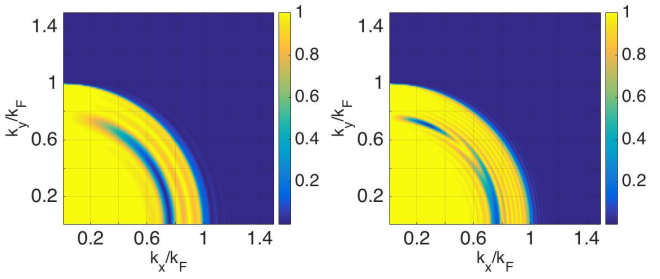

FIG. 3: Momentum occupations $|v_{\mathbf{k}}|^2$ at $t \cdot \epsilon_F = 25$ (left) and 60 (right). $1/k_F^3 a_p$ is quenched from -20 to -10.

a hole-burning ring which moves to the equator ($k_x = 0$) while another hole-burning region of smaller extent is being created on the k_x-axis.

The pairing field $|\Delta_0|$ reaches a local maximum in time domain when the momentum occupation at the hole-burning point is completely depleted (i.e. hole-burning is maximum) on the k_x-axis and reaches a local minimum when the hole-burning on the k_x-axis disappears. This agreement between the oscillation frequency of the pairing field $|\Delta_0|$ and the hole-burning frequency on the k_x-axis will be explained when the pair amplitude distribution is discussed. The frequency of the hole-burning oscillation in case (a) is $\omega \approx 0.12\epsilon_F$. Compared with a s-wave case where the hole-burning frequency is, in the narrow resonance limit, the detuning energy which is almost molecular (resonant) state energy in the weak coupling limit [3], the hole-burning frequency in the p-wave Fermi gas is much smaller than the resonant state energy: $\omega/E_r \approx 0.12$ in case (a) above.

As the final $1/k_F^3 a_p$ approaches the unitarity parametrically (even though the validity of MF description might be questionable near the unitary regime), the hole-burning point goes down following the decrease of resonant state energy E_r. When the final $1/k_F^3 a_p$ is put in BEC side ($\mu < 0$) as in case (b), there does not appear a hole-burning: a large time-scale oscillation connected to hole-burnings disappears and there remains a decaying oscillation with a short time-scale which is connected to the small dynamics near the Fermi surface of the initial state.

Next, we consider the case that the inverse scattering volume is quenched to the value of weaker attraction (hereafter, called "backward quench"): (a) BCS $\to$ BCS ($1/k_F^3 a_p$: $-10 \to -20$), (b) BEC $\to$ BCS ($1/k_F^3 a_p$: $+10 \to -15$), and (c) BEC $\to$ BEC ($1/k_F^3 a_p$: $+20 \to +5$, not shown for the same reason as in the forward quench). Figure 4 shows the dynamics of the pairing amplitude $|\Delta_0|$ and the momentum distribution $|v_{\mathbf{k}}|^2(k_z = 0)$ at the designated time. The density plots of cases (a) and (b) in Fig. 4 are displayed in Fig. 5.

When quenched to BCS regime regardless of whether the initial state is in BCS or BEC side, there appears a peak of the quasiparticle amplitude (called "particle peak") in momentum occupation $|v_{\mathbf{k}}|^2$. This is nothing but a signature of dissociation of paired atoms in (a) BCS condensate or (b) BEC via resonant state of the final Hamiltonian. In case (a), a particle peak is at $k = k_p$ satisfying $k_p^2/2M \approx \epsilon_F \approx E_r/2$ where E_r is the resonant state energy at the final value of $1/k_F^3 a_p$. The location of the particle peak is independent of the initial states with $1/k_F^3 a_p = -15$, -10, and -5 (also for $+5$ and $+20$ which belong to (b) BEC $\to$ BCS). In case (b), a quasiparticle peak is also at $k = k_p$ satisfying $k_p^2/2M \approx 0.8\epsilon_F \approx E_r/2$.

The anisotropy of the p-wave pairing field ($\Delta_{\mathbf{k}}(t) \propto \cos\theta$) makes the dissociation rate slow down as the polar angle from the k_x-axis increases: a particle peak appears on the k_x-axis at the early stage and moves to the equator while another particle peak is being created on the k_x-

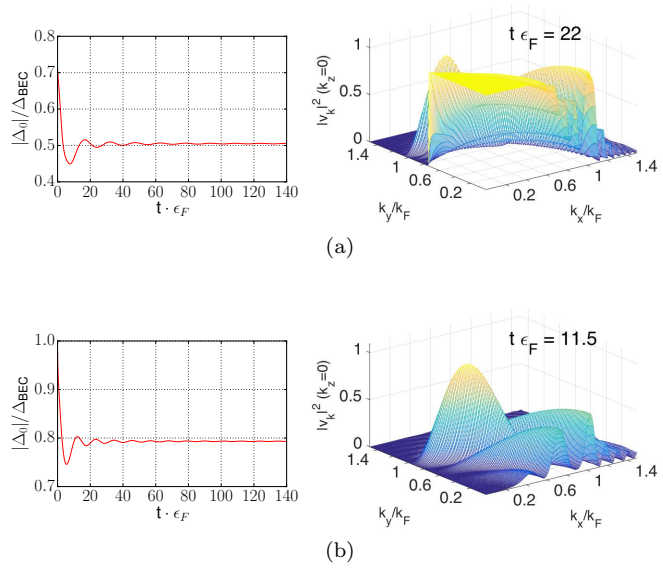

FIG. 4: Dynamics of $|\Delta_0|$ and the momentum occupation $|v_{\mathbf{k}}|^2$ at the designated time. Inverse scattering volume $1/k_F^3 a_p$ is quenched (a) from -10 to -20 and (b) from $+10$ to -15.

axis as seen in Fig. 4 and Fig. 5.

The pairing amplitude $|\Delta_0|$ reaches a local minimum in time domain when the particle peak reaches a maximum on the k_x-axis and reaches a local maximum in time domain when the particle peak disappears on the k_x-axis: the oscillation frequency of the pairing amplitude $|\Delta_0|$ agrees with that of the particle peak on the k_x-axis.

To understand the relation between the dynamics of the pairing amplitude $|\Delta_0|$ and the dynamics of quasiparticles in momentum space, a close look at the dynamics of the pair amplitudes $u^*_{\mathbf{k}} v_{\mathbf{k}}$ is helpful. Figure 6 shows the magnitude (left panel) and phase (right panel) of the pair amplitude $u^*_{\mathbf{k}} v_{\mathbf{k}}$ in momentum space in the cases of forward quench ($1/k_F^3 a_p : -20 \to -10$) and backward quenches ($1/k_F^3 a_p$: $-10 \to -20$ and $+10 \to -15$).

The hole-burning region (ring shape around the k_x-axis) off the k_x-axis has a phase rotation of 2π around the core (see the red circles in the right panels of Fig. 6) while the hole-burning region created on the k_x-axis cannot topologically. This makes the contribution of the pair amplitudes around the vortex-ring shaped region to the pairing field Δ_0 become very small because $\Delta_0 \propto \sum_{\mathbf{k}'} \Gamma_0(\mathbf{k}') u^*_{\mathbf{k}'} v_{\mathbf{k}'}$ and $\Gamma_0(\mathbf{k})$ takes similar values on the cross-sectional area of the hole-burning ring: there is a strong cancellation in the summation $\sum_{\mathbf{k}'} u^*_{\mathbf{k}'} v_{\mathbf{k}'}$ for the hole-burning region off the k_x-axis, which explains the agreement between the oscillation frequency of the pairing amplitude $|\Delta_0|$ and the hole-burning frequency on the k_x-axis. The successively created hole-burning region on the k_x-axis has smaller extent in momentum space than the previous one due to the presence of hole-burning region created off the k_x-axis (see Fig. 3) and Δ_0

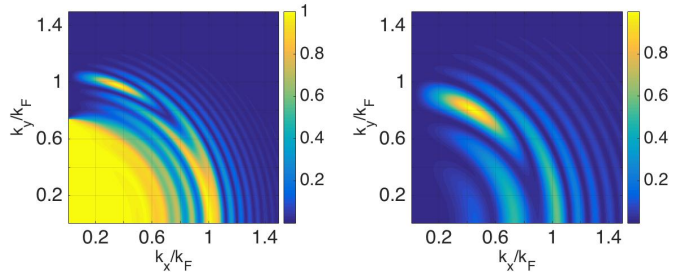

FIG. 5: The snapshots of the momentum occupation $|v_{\mathbf{k}}|^2$. $1/k_F^3 a_p$ is quenched (a) from -10 to -20 (left) and (b) from $+10$ to -15 (right).

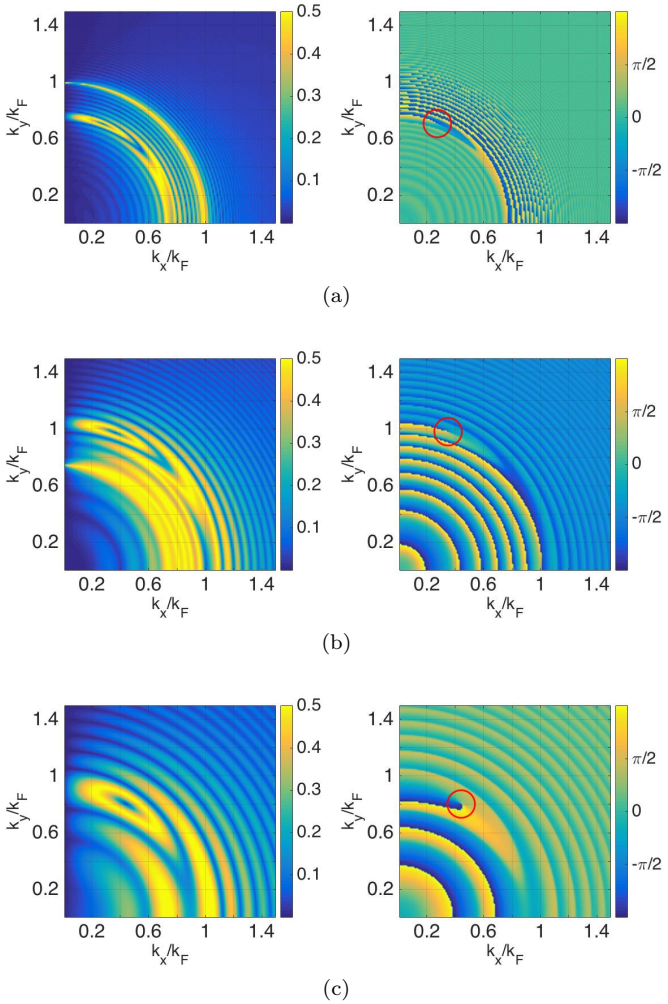

FIG. 6: The snapshots of the magnitude (left column) and the phase (right column) of the pair amplitude $u^*_{\mathbf{k}} v_{\mathbf{k}}$ in momentum space. The red circles in right panels highlight the position of the phase rotation of 2π. $1/k_F^3 a_p$ is quenched (a) from -20 to -10 (top), (b) from -10 to -20 (middle), and (c) from $+10$ to -15 (bottom). The snapshots are taken at $t \cdot \epsilon_F = 60$, 22, and 11.5, respectively.

will have a decaying amplitude in time.

A similar argument can be applied to the cases of backward quenches.

Conclusion. - The presence of resonant state in BCS side of the p-wave FR together with the anisotropy of the pairing interaction of polar states in a single-species p-wave Fermi gas results in different pairing dynamics after quantum quench compared to the s-wave case. The hole-burning/particle-peak in momentum distribution has quite distinctive dynamical behavior which can be observed in the time-of-flight experiments.

We thank A. Bulgac and T. Mizushima for the helpful discussions. This work was supported by the Max Planck Society, MEST of Korea, Gyeongsangbuk-Do, Pohang City, for the support of the JRG at APCTP, by Basic Science Research Program through NRF by MEST (Grant No. 2012R1A1A2008028), by Project Code (IBS-R024-D1). Part of the computation was supported by the National Institute of Supercomputing and Network/Korea Institute of Science and Technology Information with supercomputing resources (KSC-2013-C3-004 and KSC-2015-C3-022).

[1] A. F. Volkov and S. M. Kogan, Zh. Eksp. Teor. Fiz. **65**, 2038 (1973) [Sov. Phys. JETP **38**, 1018 (1974)].
[2] R. Barankov, L. Levitov, and B. Spivak, Phys. Rev. Lett. **93**, 160401 (2004).
[3] A. V. Andreev, V. Gurarie, and L. Radzihovsky, Phys. Rev. Lett. **93**, 130402 (2004).
[4] M. H. Szymańska, B. D. Simons, and K. Burnett, Phys. Rev. Lett. **94**, 170402 (2005).
[5] E. Yuzbashyan, O. Tsyplyatyev, and B. L. Altshuler, Phys. Rev. Lett. **96**, 097005 (2006).
[6] R. Barankov and L. Levitov, Phys. Rev. Lett. **96**, 230403 (2006).
[7] E. A. Yuzbashyan, M. Dzero, V. Gurarie, and M. S. Foster, Phys. Rev. A **91**, 033628 (2015).
[8] V. Gurarie, Phys. Rev. Lett. **103**, 075301 (2009).
[9] A. Bulgac and S. Yoon, Phys. Rev. Lett. **102**, 085302 (2009).
[10] R. Scott, F. Dalfovo, L. P. Pitaevskii, and S. Stringari, Phys. Rev. A **86**, 053604 (2012).
[11] G. E. Volovik, *The Universe in a Helium Droplet* (Oxford University Press, Oxford, 2003).
[12] J. A. Sauls, Superfluidity in the Interiors of Neutron Stars in *Timing Neutron Stars* (Kluwer Academic Press, Dordrecht, 1989), pp. 457 - 490.
[13] N. Read and D. Green, Phys. Rev. B **61**, 10267 (2000).
[14] S. Tewari, S. Das Sarma, C. Nayak, C. Zhang, and P. Zoller, Phys. Rev. Lett. **98**, 010506 (2007).
[15] V. Gurarie, L. Radzihovsky, and A. V. Andreev, Phys. Rev. Lett. **94**, 230403 (2005); V. Gurarie and L. Radzihovsky, Ann. Phys. **322**, 2 (2007).
[16] C.-H. Cheng and S.-K. Yip, Phys. Rev. Lett. **95**, 070404 (2005).
[17] C. Ticknor, C. A. Regal, D. S. Jin, and J. L. Bohn, Phys. Rev. A **69**, 042712 (2004).
[18] J. Zhang, E. G. M. van Kempen, T. Bourdel, L. Khaykovich, J. Cubizolles, F. Chevy, M. Teichmann, L. Tarruell, S. J. J. M. F. Kokkelmans, and C. Salomon, Phys. Rev. A **70**, 030702 (2004).
[19] C. H. Schunck, M. W. Zwierlein, C. A. Stan, S. M. F. Raupach, W. Ketterle, A. Simoni, E. Tiesinga, C. J. Williams, and P. S. Julienne, Phys. Rev. A **71**, 045601 (2005).
[20] J. P. Gaebler, J. T. Stewart, J. L. Bohn, and D. S. Jin, Phys. Rev. Lett. **98**, 200403 (2007).
[21] J. Fuchs, C. Ticknor, P. Dyke, G. Veeravalli, E. Kuhnle, W. Rowlands, P. Hannaford, and C. J. Vale, Phys. Rev. A **77**, 053616 (2008).
[22] J. Levinsen, N. R. Cooper, and V. Gurarie, Phys. Rev. A **78**, 063616 (2008); Y. Inada, M. Horikoshi, S. Nakajima, M. Kuwata-Gonokami, M. Ueda, and T. Mukaiyama, Phys. Rev. Lett. **101**, 100401 (2008).
[23] Z. Fu, L. Huang, Z. Meng, P. Wang, L. Zhang, S. Zhang, H. Zhai, P. Zhang, and J. Zhang, Nat. Phys. **10**, 110 (2014).
[24] T. Yamaguchi and Y. Ohashi, Phys. Rev. A **92**, 013615 (2015).
[25] C. Zhang, S. Tewari, R. M. Lutchyn, and S. Das Sarma, Phys. Rev. Lett. **101**, 160401 (2008).
[26] Y.-J. Han, Y.-H. Chan, W. Yi, A. J. Daley, S. Diehl, P. Zoller, and L.-M. Duan, Phys. Rev. Lett. **103**, 070404 (2009).
[27] N. R. Cooper and G. V. Shlyapnikov, Phys. Rev. Lett. **103**, 155302 (2009).
[28] B. Juliá-Díaz, T. Graß, O. Dutta, D.E. Chang, and M. Lewenstein, Nat. Commun. **4**, 2046 (2013).
[29] R. A. Williams, L. J. LeBlanc, K. Jiménez-García, M. C. Beeler, A. R. Perry, W. D. Phillips, and I. B. Spielman, Science **335**, 314 (2012).
[30] R. A. Williams, M. C. Beeler, L. J. LeBlanc, K. Jiménez-García, and I. B. Spielman, Phys. Rev. Lett. **111**, 095301 (2013).
[31] M. S. Foster, M. Dzero, V. Gurarie, and E. A. Yuzbashyan, Phys. Rev. B **88**, 104511 (2013); M. S. Foster, V. Gurarie, M. Dzero, and E. A. Yuzbashyan, Phys. Rev. Lett. **113**, 076403 (2014).
[32] Y. Dong, L. Dong, M. Gong, and H. Pu, Nat. Commun. **6**, 6103 (2015).
[33] M. Dzero, A. A. Kirmani, and E. A. Yuzbashyan, Phys. Rev. A **92**, 053626 (2015).
[34] T.-L. Ho and R. B. Diener, Phys. Rev. Lett. **94**, 090402 (2005).
[35] M. Iskin and C. A. R. Sá de Melo, Phys. Rev. Lett. **96**, 040402 (2006).